Transient Filling Flow into Microchannels Considering Surface Tension

Dong Sung Kim, Kwang-Cheol Lee, Tai Hun Kwon*, and Seung S. Lee

* Department of Mechanical Engineering, Pohang University of Science and Technology, San 31 Hyoja-dong Nam-gu, Pohang, Kyungbuk, 790-784, Korea, thkwon@postech.ac.kr

ABSTRACT

In this paper, we investigated, both experimentally and numerically, transient "filling" flow into microchannels, which differs from completely "filled" flow in micro-channels. An experimental flow visualization system was devised to observe the characteristics of microchannel filling flow. Microchannels were fabricated using SU-8 on the silicon substrate. A numerical analysis system has also been developed considering the surface tension effect with a contact angle concept based on the finite element method. Experimental observations show that surface tension affects significantly the filling flow that even a flow blockage phenomenon was observed. Numerical analysis system also confirms that flow blockage phenomena could take place due to the flow hindrance effect of surface tension, which is consistent with experimental observation. Experimental and numerical results in this study could be applied to design microinjection molding, micro-fluidic devices and MIMIC (micromolding in capillaries) process.

Keywords: Microchannels, Surface tension, Contact angle, Transient filling flow, Finite Element Method

1 INTRODUCTION

In order to produce precise microproducts using microinjection molding, it is required to design microcavity and microrunner rigorously based on the understanding of "filling" flow into them. Kemmann *et al.* performed the filling simulation into the microcavity using the conventional numerical analysis system [1]. They found that the melt front effects at thinner microside wall could not be predicted by usual software tools. In this regard, it is desirable to investigate the surface effects in the filling flow into microchannel.

"Filling" flow driven by surface tension, so-called flow imbibition, is a fundamental mechanism of MIMIC (micromolding in capillaries) process [2]. Kim *et al.* carried out experimental study of imbibing liquids in rectangular capillaries. They analyzed filling flow with a concept of dynamic contact angle. They showed rates of filling flow into capillary are linearly correlated to the cosine of static advancing contact angle [3]. But they did not investigate the relation between inlet pressure and surface tension with regard to the flow front advancement.

The understanding of "filling" flow is also important in microfluidic and biochemical devices. Many experimental and numerical studies of microchannel flow were performed in order to understand the microscale fluid flow in microfluidic devices [4-5]. However these studies are mostly oriented in the case of completely filled flow in microchannels. Recently Tseng *et al*. investigated fluid filling into microreservoirs [6]. They used the Volume-of-Fluid method as a numerical scheme and considered surface tension as a volumetric force of which the physical basis is not well clarified.

In this paper, the flow visualization experiments of microchannel filling flow were carried out. And a numerical simulation system was developed considering the surface tension effect to predict the filling flow into microchannels.

2 FLOW VISUALIZATION

We have performed flow visualization experiments by making use of microchannel plates of three different thickness (nominal value of 20, 30, and 40μm), with the same planar geometrical shapes as shown in Figure 1. The microchannels were made of SU-8 photoresist (Microchem Corp.) on the silicon substrate by using UV photo-lithography. The microchannel plates were designed to investigate the effects of various forces such as inertia force, shear force, pressure gradient and, in particular, surface tension. The working fluid enters into an entrance zone of 20mm × 10mm, flows through ten microchannels of different width, and finally merges to an exit zone of 20mm × 10mm. The width of ten microchannels varies from 100μm to 1mm with an increment of 100μm.

A flow visualization system established in this study is shown in Figure 2. It consists of a reservoir, a microchannel assembly, a CCD camera, a microscope, and a computer with a graphic grabber installed. The microchannel assembly is designed to place a microchannel plate at the center of jigs and prevent any leakage flow between microchannels. The jigs were made of transparent acrylic through which the filling flow into microchannel can be observed. In this study, water was used as the working fluid at laboratory temperature (15~20°C). One can vary the flow

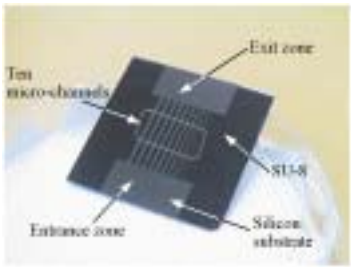

Figure 1: Fabricated microchannel plate.

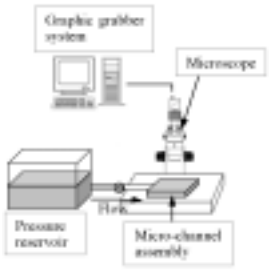

Figure 2: Schematic of experimental setup

rate by changing the pressure head via the reservoir level. The filling patterns were dynamically recorded to a computer via CCD camera and a graphic grabber system.

3 NUMERICAL ANALYSIS

3.1 Physical and numerical modeling

A micro-channel with a high width-to-thickness ratio (*thickness/width << 1*) can be modeled by thin cavity geometry. Hele-Shaw flow approximation is valid for such a geometry based on the small characteristic length [7]. On the other hand, a rectangular cross-sectioned duct could be modeled by a circular cross-sectional pipe with an equivalent hydraulic radius which might be corrected by C_{f1}. C_{f1} is a correction factor determined such that the filling time of a pressure driven filling flow in a pipe becomes the same as that in a rectangular channel derived as follows [8]:

$$C_{f1} = \sqrt{\frac{2F_p}{3}}\left(1+\frac{H}{W}\right) \tag{1}$$

where W and H are width and thickness of the rectangular duct, respectively, and F_p is a *shape factor* determined by,

$$F_p = 1 - \frac{192H}{\pi^5 W}\sum_{p=1,3,5,\cdots}\frac{1}{p^5}\tanh\frac{p\pi W}{2H} \tag{2}$$

Finite element formulation for non-Newtonian isothermal filling flow is basically the same as the previous formulation of Kim *et al.* [7] expect for including the surface tension effect and two correction factors in this particular study. As a proper boundary condition associated with entrance nodes, we introduced a prescribed pressure at entrance nodes. The flow rate through the entrance node i, Q_i, can be calculated under the assumption of a quasi-static Poiseuille flow.

3.2 Boundary condition on the flow front

In the present study, the boundary condition on the flow front is obtained via the Young-Laplace Equation in order to take into account the surface tension effect:

$$\Delta p = \sigma\left(\frac{1}{R_1}+\frac{1}{R_2}\right) \tag{3}$$

where σ is the surface tension of the fluid, R_1 and R_2 are the principal radii of curvature of flow front shape.

Surface tension effect has been introduced with the help of a dynamic contact angle instead of two principal radii of curvature as schematically depicted in Figure 3. Figure 3 shows two types of flow with regard to the surface tension effect: a pressure driven flow with a negative (flow hindrance) effect, and a surface tension driven flow with a positive (flow enhancement) effect. Depending on the positive or negative effect, the range of θ varies: $90° < \theta \le 180°$ for the negative effect, $0° \le \theta < 90°$ for the positive effect. $\theta = 90°$ is a special case when the surface tension acts no effect on the flow. Furthermore, as many researchers did [3 and 6], we assumed that contact angle remains unchanged during the entire filling flow in the present analysis.

From the geometric relations with width (W) and thickness (H) of a rectangular duct, one can determine principal radii from geometry variables as follows:

$$R_1 = -\frac{W}{2\cos\theta} \text{ and } R_2 = -\frac{H}{2\cos\theta} \tag{4}$$

For the thin cavity geometry ($W >> H$), the surface tension effect in the width direction could be neglected in comparison with that in the thickness direction since $1/R_2 >> 1/R_1$. Then Equation (4) is reduced to

$$p_{flow\ front} = -\frac{\sigma\cos\theta}{b} \tag{5}$$

where b is $H/2$.

When the rectangular channel of a relatively small width is modeled by a pipe element of an equivalent hydraulic radius, $R_{h,cor1}$ corrected by C_{f1}, i.e., $R_{h,cor1} = C_{f1}R_h$, the pressure at the flow front should be assigned by

$$p_{flow\ front} = -\frac{2\sigma\cos\theta}{R_{h,cor2}} = -\frac{2\sigma\cos\theta}{(C_{f2}/C_{f1})R_{h,cor1}} \tag{6}$$

where $R_{h,cor2}$ is the equivalent hydraulic radius of circular pipe corrected by C_{f2} as $R_{h,cor2} = C_{f2}R_h$ and C_{f2} is a

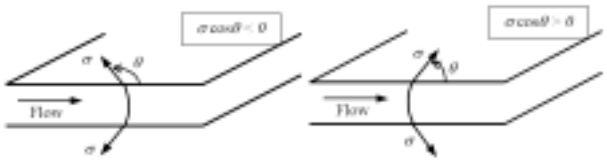

(a) (b)

Figure 3: Flow types: (a) pressure driven flow and (b) surface tension driven flow.

correction factor determined such that the filling time of a surface tension driven flow in a pipe becomes the same as that in a rectangular channel derived as follows [8].

$$C_{f2} = \frac{2}{3}\left(1+\frac{H}{W}\right)^2 F_p \tag{7}$$

4 RESULTS AND DISCUSSIONS

4.1 Experimental results

Figure 4 shows experimental results at the exit zone of the microchannels of 40μm thick and 100μm to 500μm wide for the pressure head of 30cm (Figure 4(a)) and 20cm (Figure 4(b)). For 20cm pressure head (equivalently 1.96kPa at 15.6°C), the flow hindrance in narrow channels is observed and the exit of 100μm-width channel is even blocked by a reversal flow coming from the wider channels, as indicated in Figure 4(b). With 30cm pressure head (equivalently 2.94kPa at 15.6°C), however, the block phenomenon is not observed as shown in Figure 4(a). This remarkable difference might be explained as follows. The negative effect of surface tension, flow hindrance as represented in Figure 3(a), in 100μm-width channel is becoming more dominant than that in wider channels when the inlet pressure is small enough due to the non-negligible curvature effect in the width direction, i.e., R_1 in Equation (4). It may be conjectured that the curvature effect along the width direction in the 100μm-width channel could be in a comparable order with the curvature effect in the thickness direction. It might be noted here that one should avoid such a significant defect of incomplete filling which could take place in the microinjection molding, in microfluidic devices, or in MIMIC process with multiple flow channels.

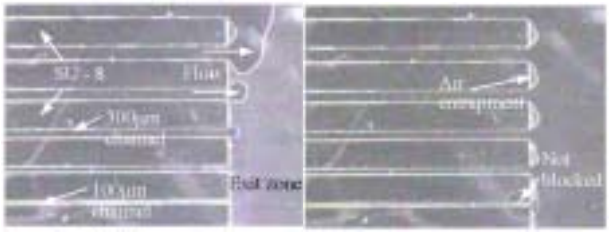

(a) 30cm pressure head (2.94kPa at 15.6°C)

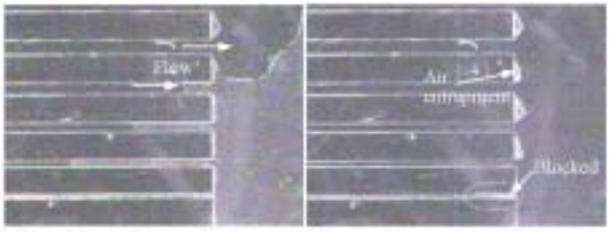

(a) 20cm pressure head (1.96kPa at 15.6°C)

Figure 4: Snap shots of filling flow at exit zone (40μm thickness) with pressure head of: (a) 30cm and (b) 20cm

4.2 Numerical and experimental results

We carried out the dimensional analysis, according to the Π-theorem, for finding important system variables based on the experimental observations. For the transient filling flow case, several variables and parameters relevant to inlet pressure (P_{in}) are as listed below:

- density (ρ), viscosity (η), and surface tension (σ) of the fluid as Material parameters, averaged flow rate $\overline{Q} = V/t_f$ (where V and t_f are total volume and total filling time, respectively) as Process variables, and half thickness of cavity (b), contact angle (θ) as Geometric variables.

From the dimensional analysis, the inlet pressure can be expressed by the following dimensionless function form:

$$\frac{P_{in}\, b}{\sigma} = f\left(\frac{\eta\,\overline{Q}}{\sigma\, b^2}, \frac{\rho\,\overline{Q}^2}{\sigma\, b^3}, \theta\right) \tag{8}$$

The relationship, Equation (8), consists of three dimensionless groups: the first term ($P_{in}\, b/\sigma$) represents dimensionless pressure; the second term ($\eta\,\overline{Q}/\sigma\, b^2$) is Capillary number (*Ca*), the ratio of viscous force to surface tension; and the last term ($\rho\,\overline{Q}^2/\sigma\, b^3$) is Weber number (*We*), the ratio of inertia force to surface tension. Another dimensionless parameter could be obtained by dividing the third one by the second one, namely Reynolds number (*Re*), which, however, does not play an important role.

We extensively performed numerical simulations by changing material properties (e.g. water and oil as a working fluids), microchannel thickness, contact angle, or inlet pressure and so on. From the numerical analysis results, a quite systematic relationship between the dimensionless pressure and *Ca* was found to be,

$$\frac{P_{in}\, b}{\sigma} \approx 3.596\,\frac{\eta\,\overline{Q}}{\sigma\, b^2} - \cos\theta \tag{9}$$

It should be noted that the linear relationship in Equation (9) is the same irrespective of fluid physical properties. With this relation, we have plotted experimental results between dimensionless pressure and *Ca* as shown in Figure 5 and the following relationship is resulted in:

$$\frac{P_{in}\, b}{\sigma} = 3.934\,\frac{\eta\,\overline{Q}}{\sigma\, b^2} + 0.053 \tag{10}$$

Similar value of the first terms in the right hand side of the Equations (9) and (10) may validate the quasi-static Poiseuille flow assumption and surface tension related

assumptions employed in the numerical study. Comparing the second terms, one can find the average contact angle of the whole filling process in experiments is about 93.0°.

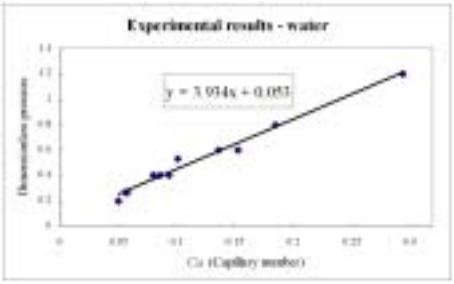

Figure 5: Relationships of dimensionless pressure and *Ca* from experimental results at lab temperature (15~20°C).

We have recognized that for a proper simulation, one must take into account the surface tension effect in the width direction as well as in the thickness direction, in particular, for 100μm-width channel. In this study, the negative effect of surface tension in the width direction was considered by modeling 100μm-width channel as a circular pipe using the equivalent hydraulic radius, corrected by C_{f1} and C_{f2}, as expressed in Equations (1) and (7).

Figures 6 and 7 show the numerical simulation results corresponding to the experimental results of Figure 4(a), and (b), respectively, with considering the negative effect of surface tension with an obtuse contact angle, $\theta = 90.7°$. The flow blockage phenomenon is predicted in the case of an inlet pressure of 1.96kPa (Figure 7), while no flow blockage is simulated in the case of 2.94kPa (Figure 6). In contrast, numerical simulation with $\theta = 90°$ did not predict the flow blockage phenomena in both cases (not shown here). Therefore one can conclude that the numerical prediction of the flow blockage in the narrowest width channel is enabled by the negative effect of surface tension, not by viscous force effect.

5 CONCLUDING REMARKS

In this paper, the flow visualization experiment and the corresponding numerical investigation for microchannel filling process have been carried out. We have designed, manufactured, and assembled the flow visualization experimental setup. A finite element analysis system was developed incorporating surface tension effect to simulate the filling flow into microchannels. Some conclusions according to our experimental and numerical results are summarized as follows:

(1) From the numerical and experimental results, it has been found that there is a linear relationship between dimensionless pressure and *Ca*, confirmed by similar slopes in numerical and experimental cases. And from the experimental results, the average contact angle of the whole filling is found to be 93.0° (the obtuse angle).

(2) Overall experimental observations (e.g. the flow hindrance and the flow blockage in narrower channels) were successfully predicted by the numerical simulation, confirming the negative effect of surface tension in pressure driven flow with the help of two correction factors, C_{f1} and

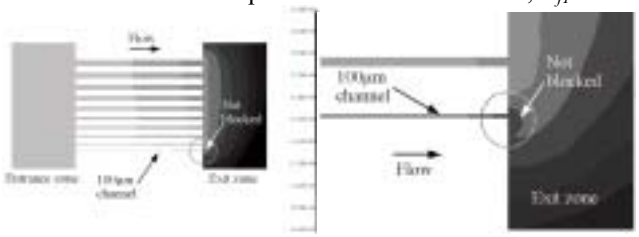

(a) (b)

Figure 6: Filling patterns corresponding to Figure 4(a): (a) overall pattern and (b) near the exit of narrower channels.

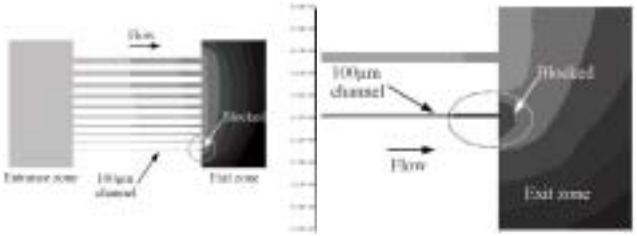

(a) (b)

Figure 7: Filling patterns corresponding to Figure 4(b): (a) overall pattern and (b) near the exit of narrower channels.

C_{f2}, and with the obtuse contact angle, $\theta = 90.7°$.

(3) The numerical method of filling flow simulation, with surface tension effect taken into account, developed in this study could be applied to design mold cavities and runner system in microinjection molding, multi-channels in microfluidic system and MIMIC process.

Acknowledgement

The authors would like to thank the National Research Laboratory Program (2000-N-NL-01-C-148) and Milli-Structure Manufacturing Technology Program for the financial supports.

REFERENCES

[1] O. Kemmann and L. Weber, Tech. Paper Ann. Tech. Meet. Conf. – SPEI, 1**,** 576-80, 2000.

[2] E. Kim, Y. Xia and G.M. Whitesides, Nature, 376, 581-84, 1995.

[3] E. Kim and G.M. Whitesides, J. Phys. Chem., 101, 855-63, 1997.

[4] I. Papautsky, J. Brazzle, T. Ameel and A.B. Frazier, Sensors Actuators A, 73, 101-08, 1999.

[5] J.I. Molho, *et al.*, MEMS ASME DSC, 66, 69-76, 1998.

[6] F.G. Tseng, *et al.*, Int. Conf. on Solid-State Sensors and Actuators, Transducers`01, 1518-21, 2001.

[7] I.H. Kim, S.J. Park, S.T. Chung and T.H. Kwon, Poly. Eng. Sci., 39, 1930-42, 1999.

[8] D.S. Kim, K.-C. Lee, T.H. Kwon and S.S. Lee, J. Micromech. Microeng., submitted.